AIMS Mathematics, 10(10): 23919–23942.
DOI: 10.3934/math.20251063
Received: 15 July 2025
Revised: 02 October 2025
Accepted: 13 October 2025
Published: 21 October 2025

https://www.aimspress.com/journal/Math

Research article

Forecasting Chinese crude oil futures volatility using dynamic volatility spillover CARR-MIDAS model

Xinyu Wu[1], Yuanzheng Liu[2], Junlin Pu[3] and Xiaona Wang[4,*]

[1] International Business School, Anhui University of Finance and Economics, Hefei 230071, China
[2] School of Finance, Anhui University of Finance and Economics, Bengbu 233030, China
[3] China School of Banking and Finance, University of International Business and Economics, Beijing 100029, China
[4] School of Finance, Tongling University, Tongling 244061, China

* **Correspondence:** Email: xiaonawang@tlu.edu.cn.

Abstract: This paper proposes a dynamic volatility spillover conditional autoregressive range-mixed data sampling (DVS-CARR-MIDAS) model to forecast volatility in the Chinese crude oil futures market by incorporating dynamic volatility spillovers from the dominant US crude oil futures market to the emerging Chinese crude oil futures market. Empirical results based on West Texas Intermediate (WTI) crude oil and Shanghai International Energy Exchange (INE) data revealed significant and time-varying spillover effects from the US to the Chinese market. In addition, the DVS-CARR-MIDAS model consistently showed that the proposed model consistently outperforms benchmark models in both in-sample fitting and out-of-sample forecasting. These findings were robust to the Diebold-Mariano (DM) test, R^2_{oos} test, alternative dominant market, and different out-of-sample forecast windows. Furthermore, the economic value analysis demonstrated that the proposed model provides meaningful benefits for portfolio management.

Keywords: volatility forecasting; dynamic volatility spillover; DVS-CARR-MIDAS; crude oil market
Mathematics Subject Classification: 62M10, 91B84, 91G20

1. Introduction

Crude oil has always been a vital component of the global energy system, serving not only as a fundamental fuel source but also as a strategic commodity that exerts profound influence over macroeconomic and financial dynamics. Its price volatility affects a wide array of economic outcomes, including inflation rates, monetary policy transmission, investment allocation, asset pricing, and overall financial stability, thereby highlighting the necessity of precise volatility measurement and

modeling [1, 2]. As the global energy market becomes increasingly interconnected, the Chinese crude oil futures market has increasingly aligned with international markets, enhancing China's role in energy pricing and risk management. This trend reflects China's rising role in global commodity markets but also introduces greater vulnerability to external shocks and market contagion [3].

Numerous studies have shown that shocks originating from major global benchmarks like West Texas Intermediate (WTI) and Brent Crude are transmitted into the Chinese crude oil futures market, with China primarily functioning as a recipient in the spillover network. Specifically, Liu and Lee [4] demonstrated that the Shanghai International Energy Exchange (INE) crude oil futures market is strongly affected by global financial uncertainty and exhibits asymmetric connectedness with WTI and Brent. Using a time-varying parameter vector autoregression (VAR) model, Sun et al. [5] showed that China's crude oil futures primarily serve as a net information receiver in global crude oil and spot markets, although their transmitting role has slightly increased in recent years. From a time-varying perspective, Su and Lin [6] also found that Shanghai crude oil futures consistently act as a net receiver of price information from international benchmarks, with their pricing influence strengthening gradually after 2021. These spillover effects are closely tied to extreme events such as geopolitical tensions and financial crises, all of which can induce large and sudden shifts in crude oil price dynamics [3, 7]. Recognizing and modeling these transmission effects is essential for accurately forecasting volatility in the Chinese crude oil futures market.

Crucially, these cross-market spillover effects are not stable over time. Recent studies have identified substantial time variation in both the magnitude and direction of volatility transmission. For instance, Yang et al. [8] utilized asymmetric VAR connectedness networks to demonstrate that spillover effects are state-dependent and shift over time, particularly during periods of heightened uncertainty. Similarly, Huang and Huang [9] showed that the intensity of spillovers fluctuates across different investment horizons, reflecting distinct mechanisms in short- and long-term transmission. These findings underscore the need for models that go beyond static linear assumptions to capture both dynamic interdependence and potential structural changes in volatility regimes.

Meanwhile, a growing strand of literature has focused on modeling time-varying volatility spillovers using frameworks such as dynamic connectedness networks, time-varying parameter vector autoregressions (TVP-VAR), and multivariate generalized autoregressive conditional heteroskedasticity (GARCH) models. For instance, Li et al. [10] employed both static and dynamic connectedness approaches to examine return and volatility spillovers between China's crude oil futures market and green energy equity sectors, finding that the dominance structure of volatility transmission evolves over time and is significantly affected by external shocks such as the COVID-19 pandemic and the launch of China's carbon trading market. Similarly, Dai and Zhu [11] utilized a TVP-VAR model to analyze volatility interactions among WTI crude oil, natural gas futures, and various Chinese stock indices, revealing substantial spillover variability and regime shifts during crisis episodes. Building on frequency-domain analysis, Jin et al. [12] employed the Baruník-Křehlík (BK) spectral decomposition approach to show that spillover effects among geopolitical risk, climate risk, and energy markets are not only significant but also highly frequency-dependent, with high-frequency components being particularly sensitive to geopolitical tensions. In parallel, Salem et al. [13] used the dynamic conditional correlation (DCC) GARCH-connectedness framework to capture the time-varying volatility transmission between oil prices and major exchange rates, offering insights into the co-movement and dynamic hedging behavior under market uncertainty.

These approaches have significantly advanced our understanding of dynamic interdependence. However, most of them rely exclusively on close-to-close return data. As a result, they tend to neglect the rich intraday information embedded in the price range, which may provide more accurate and timely signals of market uncertainty.

To improve the utilization of information, range-based volatility estimators have been proposed. These estimators rely on the daily high-low price range and provide a more efficient and timely proxy for volatility under standard assumptions. Parkinson [14] was among the first to show that range-based measures outperform squared returns in estimating true volatility. Building on this insight, Chou [15] introduced the conditional autoregressive range (CARR) model, which models the conditional expectation of price ranges and has shown empirically superior forecasting performance relative to traditional GARCH models. Similarly, He et al. [16] showed that CARR-based and interval-valued models outperform GARCH-type models in forecasting the volatility and directional movement of crude oil prices, further reinforcing the practical value of range-based volatility models. Moreover, recent extensions of the CARR framework focus on enhancing its flexibility and multivariate modeling capabilities. Wang et al. [17] proposed the functional coefficient autoregressive range (FCARR) model, which incorporates varying coefficient functions to better capture nonlinear dynamics and asymmetries in financial volatility. Using Bayesian P-spline estimation, their simulation and empirical results–based on Chinese stock market data–demonstrate the model's ability to adapt to complex fluctuation patterns. In a separate study, Tan et al. [18] introduced a multivariate CARR (MCARR) and a two-stage MCARR-return framework to jointly estimate volatilities, correlations, and returns across US equity indices. Their models outperform traditional alternatives in both in-sample fit and out-of-sample forecasting.

Among the extensions of the CARR framework, the CARR mixed data sampling (CARR-MIDAS) model has attracted growing attention for its ability to integrate high-frequency range-based volatility measures with low-frequency macro-financial variables. By combining the CARR model with the mixed data sampling (MIDAS) approach, the CARR-MIDAS model offers a parsimonious yet flexible structure for capturing multi-scale drivers of volatility and has been shown to improve forecasting performance. Recent studies have explored the incorporation of additional macro-financial variables. For example, Wu et al. [19] incorporated time-varying risk aversion into the CARR-MIDAS model to forecast renminbi exchange rate volatility, finding that the model delivers more accurate forecasts than several competing approaches. Similarly, Wu et al. [20] integrated economic policy uncertainty (EPU) indices into the CARR-MIDAS framework to predict WTI crude oil futures volatility, showing that the model incorporating EPU indices significantly improve volatility forecasts.

Furthermore, while range-based models like the CARR and its MIDAS extensions have significantly improved the accuracy and flexibility of volatility forecasting by incorporating intraday price information, further methodological refinements are needed to capture time-varying cross-market spillovers. To date, few studies have integrated time-varying cross-market volatility spillovers into the CARR modeling framework. In addition, a growing body of studies has shown that structural breaks in financial return volatility are widespread in financial markets. Ignoring such structural breaks may lead to an overestimation of volatility persistence, a misclassification of volatility regimes, and a failure to adequately capture volatility spillovers across different regimes. In particular, WTI crude oil futures, as one of the most important derivatives in the global oil market, are highly sensitive to major economic and political events. These events can trigger significant changes in volatility regimes, leading to

structural breaks in volatility dynamics. Therefore, explicitly accounting for potential structural breaks in the volatility of the WTI crude oil futures market is crucial for accurately capturing cross-market dynamic volatility spillovers and enhancing market risk management.

To address this limitation, we extend the standard CARR-MIDAS framework by allowing the spillover effect to vary across structural regimes. These regimes are externally identified using the iterated cumulative sum of squares (ICSS) algorithm applied to the dominant US market, enabling the model to capture dynamic volatility spillovers from the US crude oil futures market to the Chinese crude oil futures market. Empirical studies have demonstrated its effectiveness across diverse financial contexts. For instance, Vo and Tran [21] applied the ICSS-augmented EGARCH model to detect excessive volatility shifts when analyzing spillovers from the US to ASEAN equity markets, highlighting its role in improving volatility forecast accuracy under structural instability. Similarly, Vuong et al. [22] used a modified ICSS-EGARCH framework to examine volatility transmission from China to the US during the COVID-19 pandemic, showing that the inclusion of volatility breakpoints allows for a better characterization of cross-market contagion episodes.

This paper investigates the modeling and forecasting of volatility in the Chinese crude oil futures market by incorporating range-based volatility measures and dynamic volatility spillovers. By doing so, this paper contributes to the literature in several aspects. First, we extend the CARR-MIDAS framework by allowing the spillover coefficient to vary across structural regimes identified from the US market, thereby capturing dynamic spillover effects. Second, empirical results show that spillovers from the US to China are both statistically significant and time-varying, improving the model's in-sample fit. Third, in out-of-sample forecasting, the proposed model consistently outperforms benchmark alternatives, with robustness confirmed by DM and R^2_{oos} tests across different forecast windows and alternative dominant markets. In addition, we assess the economic value of these forecasts in portfolio allocation, confirming that more accurate volatility predictions provide practical benefits for investors.

The remainder of this paper is organized as follows: Section 2 introduces the DVS-CARR-MIDAS model, the ICSS algorithm, the estimation methodology, and the forecast evaluation method. Section 3 presents the data, empirical results, and robustness checks. Section 4 concludes the study.

2. Methodology

2.1. The range

To capture crude oil futures' market volatility, we employ the intraday range proposed by Parkinson [14]. The intraday range R_t on day t is defined as

$$R_t = \frac{\log(H_t) - \log(L_t)}{\sqrt{4\log(2)}}, \tag{2.1}$$

where H_t and L_t denote the highest and lowest prices of the asset in the trading day.

2.2. The CARR model

The CARR model, originally proposed by Chou [15], provides a natural framework for modeling volatility dynamics using the intraday high-low price range rather than squared returns. Similar in

spirit to the GARCH model, the CARR specification captures persistence in conditional volatility while ensuring positivity and stationarity.

The CARR (1,1) process is defined as

$$R_t = \lambda_t \varepsilon_t, \quad \varepsilon_t \mid \mathscr{F}_{t-1} \sim \exp(1), \tag{2.2}$$

$$\lambda_t = \omega + \alpha R_{t-1} + \beta \lambda_{t-1}, \tag{2.3}$$

where R_t denotes the intraday range on day t, λ_t is its conditional expectation given the past information set $\mathscr{F}_{t-1}$, and ε_t follows a unit-mean exponential distribution. The parameter restrictions $\omega > 0$, $\alpha \geq 0$, $\beta \geq 0$, and $\alpha + \beta < 1$ guarantee that the conditional mean is positive and that the process is covariance stationary.

Compared with return-based GARCH models, the CARR model exploits the intraday range, which is a more efficient estimator of daily volatility under log-normal price dynamics. This property makes the CARR model particularly suitable for analyzing futures markets, where range-based measures capture high-frequency price variability with reduced noise.

2.3. The CARR-MIDAS model

The CARR-MIDAS model extends the basic CARR specification by decomposing the conditional mean of the range into short- and long-run components. The short-run dynamics are captured by a CARR (1,1) process, while the long-run component is driven by lagged realized range volatility (RRV) through a MIDAS regression structure. The CARR-MIDAS model is specified as follows:

$$R_t = \lambda_t \varepsilon_t, \quad \varepsilon_t \mid \mathscr{F}_{t-1} \sim \exp(1), \tag{2.4}$$

$$\lambda_t = g_t \tau_t, \tag{2.5}$$

$$g_t = (1 - \alpha - \beta) + \alpha \frac{R_{t-1}}{\tau_{t-1}} + \beta g_{t-1}, \tag{2.6}$$

$$\log(\tau_t) = m + \theta \sum_{k=1}^{K} \varphi_k(\gamma) \log(\mathrm{RRV}_{t-k}), \tag{2.7}$$

where λ_t is the conditional mean of the intraday range, decomposed into a short-term component g_t and a long-term component τ_t.

The long-run component τ_t depends on the RRV, defined as a rolling sum of past squared ranges:

$$\mathrm{RRV}_t = \sum_{i=1}^{22} R_{t-i}^2, \tag{2.8}$$

which smooths high-frequency variability and provides a persistent measure of volatility dynamics. The weights $\varphi_k(\gamma)$ in the MIDAS structure follow a one-parameter beta polynomial:

$$\varphi_k(\gamma) = \frac{(1 - k/K)^{\gamma - 1}}{\sum_{j=1}^{K} (1 - j/K)^{\gamma - 1}}, \tag{2.9}$$

where K denotes the number of lags. This functional form guarantees $\sum_{k=1}^{K} \varphi_k(\gamma) = 1$ and parsimoniously allocates decaying weights to past observations. In this paper, we set $K = 66$, corresponding to three months of lagged daily observations.

2.4. The VS-CARR-MIDAS model

The VS-CARR-MIDAS model extends the CARR-MIDAS by allowing volatility spillovers from a dominant market to a following market. In this framework, the dominant market is first modeled with a standard CARR-MIDAS, and its conditional mean serves as an input into the following market. The spillover coefficient is assumed constant across the sample period.

2.4.1. The intraday range process for the dominant (US) market

It is assumed that the intraday range of the dominant US market follows the dynamic process as follows:

$$R_{d,t} = \lambda_{d,t}\varepsilon_{d,t}, \quad \varepsilon_{d,t} \mid \mathscr{F}_{d,t-1} \sim \exp(1), \tag{2.10}$$

$$\lambda_{d,t} = \tau_{d,t}g_{d,t}, \tag{2.11}$$

$$g_{d,t} = (1 - \alpha_d - \beta_d) + \alpha_d \frac{R_{d,t-1}}{\tau_{d,t-1}} + \beta_d g_{d,t-1}, \tag{2.12}$$

$$\log(\tau_{d,t}) = m_d + \theta_d \sum_{k=1}^{K_d} \varphi_k(\gamma_d) \log(\mathrm{RRV}_{d,t-k}), \tag{2.13}$$

where $R_{d,t}$ is the daily range of the dominant market, and the MIDAS structure, including the decomposition of $\lambda_{d,t}$, the weighting function $\varphi_k(\gamma_d)$, and the definition of $\mathrm{RRV}_{d,t}$, is specified as in the CARR-MIDAS model introduced earlier (see Section 2.3).

2.4.2. The intraday range process for the emerging (Chinese) market

Similar to the dominant market, the intraday range of the Chinese crude oil futures is modeled within the CARR-MIDAS framework. The key difference is that, in addition to its own past information, the Chinese market is also influenced by the volatility spillovers from the dominant US market. The process is specified as follows:

$$R_{f,t} = \lambda_{f,t}\varepsilon_{f,t}, \quad \varepsilon_{f,t} \mid \mathscr{F}_{f,t-1} \sim \exp(1), \tag{2.14}$$

$$\lambda_{f,t} = \tau_{f,t}g_{f,t}, \tag{2.15}$$

$$g_{f,t} = (1 - \alpha_f - \beta_f) + \alpha_f \frac{R_{f,t-1}}{\tau_{f,t-1}} + \beta_f g_{f,t-1} + \kappa\lambda_{d,t-1}, \tag{2.16}$$

$$\log(\tau_{f,t}) = m_f + \theta_f \sum_{k=1}^{K_f} \varphi_k(\gamma_f) \log(\mathrm{RRV}_{f,t-k}), \tag{2.17}$$

where κ denotes the constant volatility spillover effect from the dominant market to the following market. $\lambda_{d,t}$ is the conditional range mean of the dominant market. All other parameters follow the same definitions as in the CARR-MIDAS model.

2.5. The DVS-CARR-MIDAS model

While the VS-CARR-MIDAS model provides a useful framework by incorporating a constant volatility spillover effect from the dominant (US) market to the emerging (Chinese) market, it assumes

that the spillover intensity remains unchanged over the entire sample period. This assumption may be restrictive in practice, since structural breaks or market regime shifts can lead to substantial time variation in the degree of cross-market volatility transmission.

To address this limitation, we propose the DVS-CARR-MIDAS model. As in the VS-CARR-MIDAS specification, the dominant market is modeled using a standard CARR-MIDAS specification, and its conditional range mean enters the emerging market equation as the channel of spillover. The key innovation is that the spillover coefficient is allowed to vary across structural regimes, thereby capturing potential changes in spillover dynamics over time. Specifically, the intraday range process for the emerging (Chinese) market is specified as

$$R_{f,t} = \lambda_{f,t}\varepsilon_{f,t}, \quad \varepsilon_{f,t} \mid \mathscr{F}_{f,t-1} \sim \exp(1), \tag{2.18}$$

$$\lambda_{f,t} = \tau_{f,t}g_{f,t}, \tag{2.19}$$

$$g_{f,t} = (1 - \alpha_f - \beta_f) + \alpha_f \frac{R_{f,t-1}}{\tau_{f,t-1}} + \beta_f g_{f,t-1} + \sum_{j=1}^{m} \kappa_j \text{Break}_j \lambda_{d,t-1}, \tag{2.20}$$

$$\log(\tau_{f,t}) = m_f + \theta_f \sum_{k=1}^{K_f} \varphi_k(\gamma_f) \log(\text{RRV}_{f,t-k}), \tag{2.21}$$

where κ_j represents the volatility spillover effect from the dominant US market to the emerging Chinese market during the period between breakpoints $(j-1)$ and j. The dummy variable Break_j equals 1 if time t falls within the j-th regime, and is 0 otherwise. The regime-specific nature of κ_j allows the spillover intensity to vary across structurally segmented periods, with breakpoints exogenously identified using the ICSS algorithm described in the next subsection. All other parameters are defined analogously to those in the VS-CARR-MIDAS model.

It is worth noting that the proposed specification is highly flexible, as it nests several existing models as special cases. Specifically, when κ_j is set to a constant, the model reduces to the VS-CARR-MIDAS model. When $\kappa_j = 0$, it reduces to the CARR-MIDAS model. When $\kappa_j = 0$ and $\theta_f = 0$ simultaneously, it further simplifies to the basic CARR model.

2.6. ICSS algorithm

To detect structural changes in the volatility of the dominant market, we apply the ICSS algorithm proposed by Inclan and Tiao [23] into the DVS-CARR-MIDAS framework. The ICSS algorithm identifies structural variance shifts in a time series by examining the cumulative behavior of squared residuals. It assumes that the variance remains constant within each regime but may shift abruptly at unknown breakpoints.

Let T denote the total number of observations in the sample, and let m represent the number of identified breakpoints, occurring at times $S_1 < S_2 < \cdots < S_m$. The intraday range series (e.g., WTI intraday ranges) can thus be described as

$$\text{var}(r_t^{US}) = \begin{cases} \lambda_0, & 1 < t \le S_1, \\ \lambda_1^2, & S_1 < t \le S_2, \\ \quad \vdots & \quad \vdots \\ \lambda_m^2, & S_m < t \le T. \end{cases} \tag{2.22}$$

To locate these breakpoints, the ICSS algorithm calculates the cumulative sum of squared residuals up to each time point j:

$$SS_j = \sum_{t=1}^{j} e_t^2, \tag{2.23}$$

where $j = 1, 2, \ldots, T$, and e_t represents the residual at time t. The total sum of squares over the entire sample is denoted as SS_T. The test statistic is defined as

$$D_j = \frac{SS_j}{SS_T} - \frac{j}{T}, \tag{2.24}$$

where $D_0 = D_T = 0$, i.e., the test statistic is inherently zero at the start and end of the series. If there is no change in the unconditional variance, the test statistic D_j will fluctuate mildly around zero. Under the null hypothesis of constant variance, the statistic D_j are expected to oscillate within predefined lower and upper bounds, which serve as the critical values. In other words, if the absolute value of D_j exceeds the critical threshold, the null hypothesis of no variance break is rejected. The procedure is then applied iteratively to each identified segment to detect additional breakpoints.

2.7. Maximum likelihood estimation

The DVS-CARR-MIDAS model can be estimated using the quasi-maximum likelihood method. We assume that the conditional distributions of $\varepsilon_{d,t}$ and $\varepsilon_{f,t}$ follow a simple exponential distribution. Under this assumption, the log-likelihood function is given by

$$\ell(R; \Theta) = -\sum_{t=1}^{T} \sum_{i=1}^{N_t} \left[\log(\lambda_{d,t}) - \frac{R_{d,t}}{\lambda_{d,t}} + \log(\lambda_{f,t}) - \frac{R_{f,t}}{\lambda_{f,t}} \right], \tag{2.25}$$

where $\Theta = (m_d, \theta_d, \gamma_d, \alpha_d, \beta_d, m_f, \theta_f, \gamma_f, \alpha_f, \beta_f, \kappa_f)'$ represents the vector of parameters to be estimated. The quasi-maximum likelihood estimators, denoted as $\widehat{\Theta}$, are obtained by maximizing the log-likelihood function in Eq (2.25):

$$\hat{\Theta} = \arg\max_{\Theta} \ell(\Theta). \tag{2.26}$$

2.8. Evaluation of volatility forecasting performance

2.8.1. Loss functions

We adopt four standard loss functions to evaluate out-of-sample forecast accuracy: mean absolute error (MAE), mean squared error (MSE), mean absolute percentage error (MAPE), and quasi-likelihood (QLIKE). These metrics collectively assess absolute deviation, relative error, squared error, and likelihood-based loss. The loss functions are defined as follows:

$$\text{MAE:} \quad \text{Loss}_t(\lambda_t, \hat{\lambda}_t) = \frac{1}{T} \sum_{t=1}^{T} \left| \hat{\lambda}_t - \lambda_t \right|, \tag{2.27}$$

$$\text{MSE:} \quad \text{Loss}_t(\lambda_t, \hat{\lambda}_t) = \frac{1}{T} \sum_{t=1}^{T} \left(\hat{\lambda}_t - \lambda_t \right)^2, \tag{2.28}$$

$$\text{MAPE:} \quad \text{Loss}_t(\lambda_t, \hat{\lambda}_t) = \frac{1}{T}\sum_{t=1}^{T}\left|\frac{\hat{\lambda}_t - \lambda_t}{\lambda_t}\right|, \tag{2.29}$$

$$\text{QLIKE:} \quad \text{Loss}_t(\lambda_t, \hat{\lambda}_t) = \frac{1}{T}\sum_{t=1}^{T}\left(\log\hat{\lambda}_t + \frac{\lambda_t}{\hat{\lambda}_t}\right), \tag{2.30}$$

where $\hat{\lambda}_t$ denotes the forecasted volatility and λ_t the realized volatility at time t.

2.8.2. MCS test

To evaluate the statistical significance of differences in forecasting performance across competing volatility models, we adopt the model confidence set (MCS) procedure proposed by Hansen et al. [24]. This approach identifies a subset of models that exhibit superior predictive ability by applying a sequence of hypothesis tests and an iterative elimination rule. Let $\mathcal{M}^0$ denote the initial pool of candidate models. The core of the MCS procedure is an equivalence test for equal predictive accuracy, formulated as

$$H_{0,\mathcal{M}} : \mathbb{E}(d_{uv,t}) = 0, \quad \forall u, v \in \mathcal{M}, \quad \mathcal{M} \subseteq \mathcal{M}^0, \tag{2.31}$$

where $d_{uv,t} = \text{Loss}_t(u) - \text{Loss}_t(v)$ represents the loss differential between model u and model v at time t.

To test $H_{0,\mathcal{M}}$, we employ the range statistic:

$$T_{\mathcal{M}} = \max_{u,v\in\mathcal{M}} |t_{uv}|, \tag{2.32}$$

where $t_{uv} = \frac{\bar{d}_{uv}}{\sqrt{\widehat{\text{Var}}(\bar{d}_{uv})}}$, $\bar{d}_{uv} = \frac{1}{n}\sum_{t=1}^{n} d_{uv,t}$, and $\widehat{\text{Var}}(\bar{d}_{uv})$ is a bootstrap estimate of the variance of $\bar{d}_{uv}$.

If the null hypothesis is rejected, the model with the poorest relative performance is removed. Specifically, the elimination rule is defined as

$$e_{\mathcal{M}} = \arg\max_{u\in\mathcal{M}} \sup_{v\in\mathcal{M}} t_{uv}. \tag{2.33}$$

This iterative process continues until the null hypothesis of equal predictive ability cannot be rejected for the remaining models.

The final subset of models, for which predictive accuracy cannot be statistically distinguished, constitutes the MCS. We implement the MCS using a block bootstrap procedure with 10,000 replications and set the significance level at 10%.

3. Empirical analysis

3.1. Data

This study employs the DVS-CARR-MIDAS model to capture the dynamic volatility spillover effects from the dominant US crude oil futures market to the emerging Chinese market and evaluates their implications for volatility modeling and forecasting. Given the dominant role of the US crude oil market in global energy trading [9, 25], we use the WTI crude oil futures as a proxy for the dominant US crude oil futures market. Correspondingly, we use crude oil futures traded on the Shanghai INE to represent the Chinese market. The sample covers the period from May 1, 2018, to May 1, 2025,

yielding a total of 1627 trading days during which both markets were open. All data are obtained from the Wind database.

Figure 1 displays the time series plots of daily ranges for the WTI and INE crude oil futures markets. As shown, both series of daily ranges exhibit classic features of financial time series, such as time-varying volatility and volatility clustering. Table 1 reports descriptive statistics for the WTI and INE daily ranges series. All series exhibit positive skewness and excess kurtosis, indicating fat-tailed distributions. The Jarque-Bera test results indicate that none of the series follow a normal distribution. To assess serial correlation, we apply the Ljung-Box Q test up to 20 lags. The results reveal strong persistence in the daily ranges series.

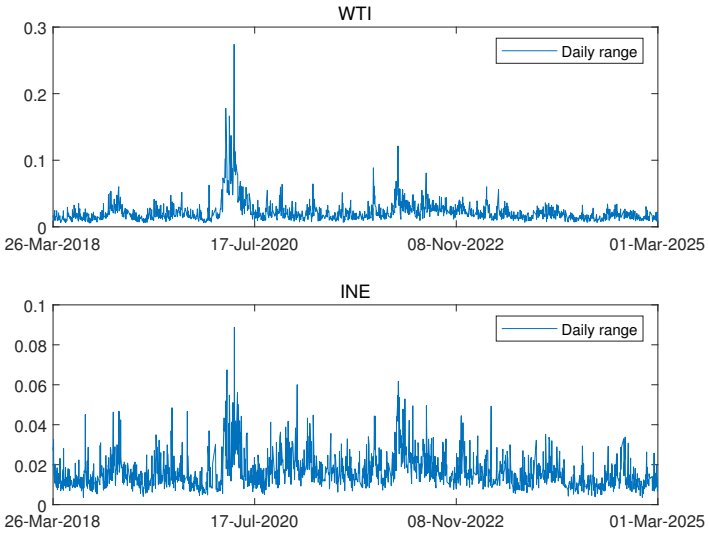

Figure 1. Daily ranges of WTI and INE crude oil futures.

Table 1. Daily range summary statistics.

	Mean	**Min**	**Max**	**Std**	**Skewness**	**Kurtosis**	**Jarque-Bera**	**Q(20)**
INE	0.0165	0.0036	0.0888	0.0088	1.9960	9.6036	4036.6403	2618.7736
WTI	0.0220	0.0055	0.2739	0.0169	5.5244	55.0574	191989.1480	7338.8062

Note: Q(20) is the Ljung-Box statistic for autocorrelation up to 20 lags.

Moreover, to account for potential structural shifts in volatility, we apply the ICSS algorithm to the WTI return series. Figure 2 graphically presents the structural breakpoints in the volatility of WTI crude oil ranges, as identified by the ICSS algorithm. The red vertical lines represent the timing of structural breaks. Specifically, the ICSS algorithm detects nine structural breaks, occurring on dates such as 2018-11-09 (Break ID 1), 2020-03-05 (Break ID 3), and 2025-02-28 (Break ID 9), among others. These breakpoints mark significant shifts in volatility dynamics, often aligned with major macroeconomic or energy-related events. For clarity, Table 2 summarizes the break dates and their corresponding identifiers, which define the structural regimes across which the volatility spillover effects are estimated. Additionally, the table reports the range-based volatility for each regime, capturing the level of market fluctuation within each structural segment. The results indicate

considerable variation in volatility intensity across regimes. For example, Regime 4 (2020-03-06 to 2020-05-07) exhibits the highest average volatility (0.0693). In contrast, periods such as Regime 9 (2024-02-03 to 2025-02-28) show substantially lower volatility (0.0146), suggesting relatively calm market conditions. This variation underscores the need for a regime-specific modeling approach in capturing dynamic volatility spillovers.

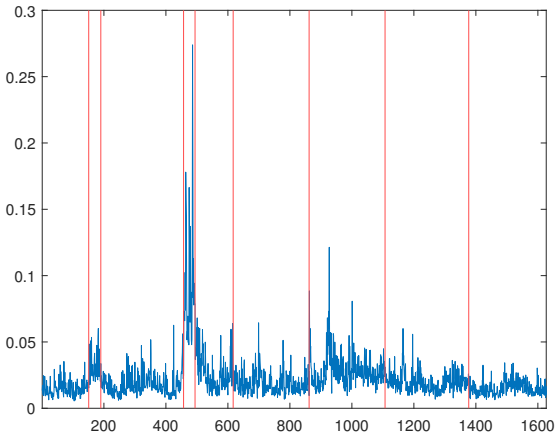

Figure 2. Volatility breakpoints in the WTI ranges identified by the ICSS algorithm.

Table 2. Break dates identified by the ICSS algorithm.

Break ID	Regime period	Range-based volatility
1	2018-05-01 – 2018-11-09	0.0138
2	2018-11-10 – 2019-01-09	0.0274
3	2019-01-10 – 2020-03-05	0.0159
4	2020-03-06 – 2020-05-07	0.0693
5	2020-05-08 – 2020-11-11	0.0377
6	2020-11-12 – 2021-11-24	0.0178
7	2021-11-25 – 2022-12-12	0.0320
8	2022-12-13 – 2024-02-02	0.0216
9	2024-02-03 – 2025-02-28	0.0146

3.2. Estimation results

We estimate the CARR, CARR-MIDAS, VS-CARR-MIDAS, and DVS-CARR-MIDAS models using the maximum likelihood. Figure 3 presents the in-sample estimates of conditional range ($\lambda_{f,t}$) for each model. Overall, all models demonstrate a reasonable ability to capture the volatility dynamics of China's crude oil futures market. For instance, each model successfully captures periods of elevated volatility, such as during the COVID-19 outbreak in 2020.

Table 3 reports the parameter estimates obtained using the quasi-maximum likelihood estimation method. Across all models, the persistence parameter, defined as $\alpha + \beta$, is generally close to one, indicating strong volatility clustering in China's crude oil market. Additionally, a similarly high level of persistence is observed for the US market in the CARR-MIDAS specification.

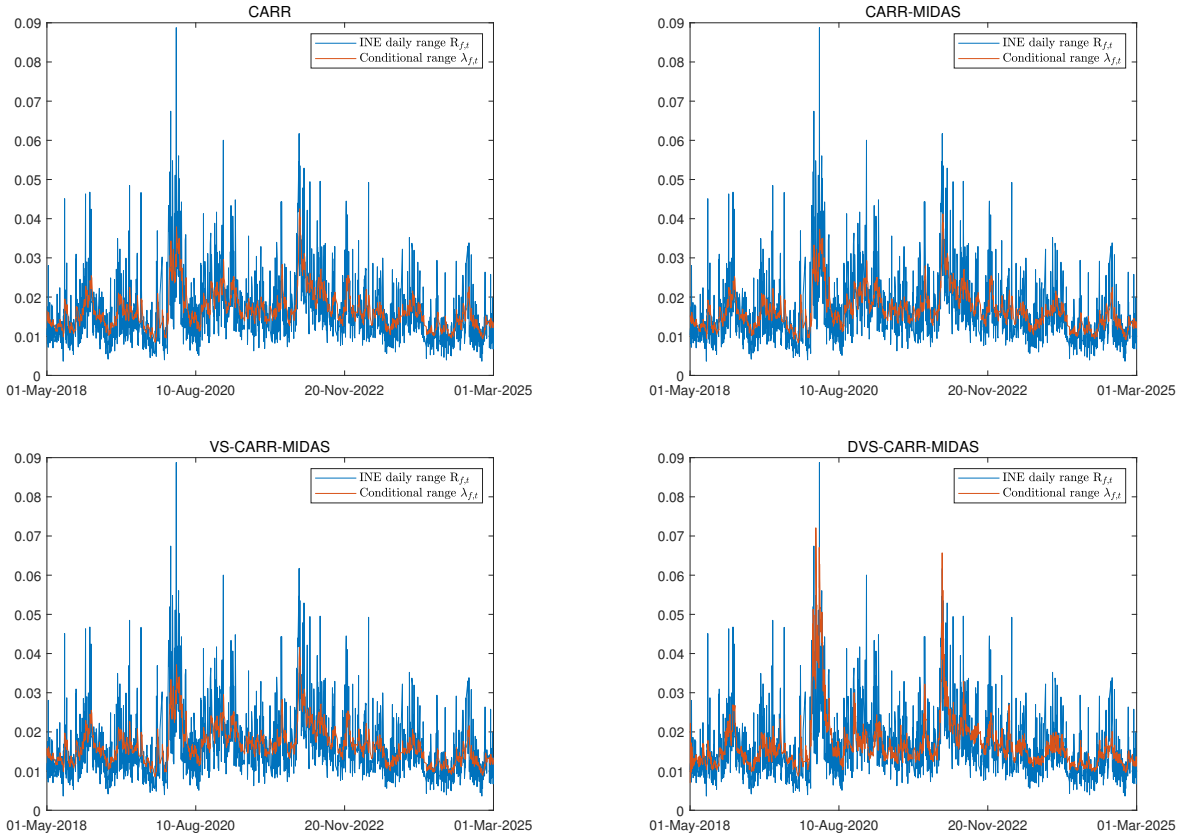

Figure 3. In-sample estimates of conditional variance for China's crude oil market.

Table 3. Parameter estimation results.

	CARR	CARR-MIDAS	VS-CARR-MIDAS	DVS-CARR-MIDAS	
		Chinese		US	Chinese
ω	6.1726E-04	-2.9970	-1.9525	-5.3965	-1.6069
	(5.6344E-04)	(0.1019)	(0.0683)	(0.3045)	(0.0745)
θ		0.2693	0.5648	-0.3847	0.5939
		(0.0315)	(0.0235)	(0.0484)	(0.0284)
γ		24.0647	6.4124	14.9929	5.0276
		(1.3731)	(0.3407)	(0.8534)	(0.2544)
β	0.7892	0.8682	0.6257	0.6618	0.7241
	(0.0431)	(0.0464)	(0.0615)	(0.0517)	(0.0685)
α	0.1734	0.1007	0.1312	0.3026	0.1396
	(0.0392)	(0.0361)	(0.0522)	(0.0460)	(0.0493)
κ			2.5205		
			(0.3286)		
Log-lik	5035.0501	5035.1492	5035.7714	4647.9950	5047.54

Note: Log-lik stands for the log-likelihood and the numbers in parentheses are the asymptotic standard errors.

In the MIDAS-augmented models, the estimated θ parameter is significantly positive across all specifications, indicating that monthly RRV provides useful information for capturing long-term volatility dynamics in the Chinese market.

In addition, the estimated volatility spillover coefficient in the VS-CARR-MIDAS model, $\kappa = 2.5205$, is positive and statistically significant. This indicates that volatility spillovers from the dominant US market exert a strong and persistent amplifying effect on China's crude oil futures market when the spillover intensity is assumed to be constant. While this provides initial evidence of cross-market volatility transmission, the static nature of κ in this specification limits the model's ability to account for structural changes over time. This limitation motivates the introduction of the DVS-CARR-MIDAS model, which allows spillover effects to vary across regimes defined by exogenous structural breakpoints.

Figure 4 illustrates the decomposition of $\lambda_{f,t}$ into its long-run component (τ_f, t) and short-run component $(g_{f,t})$ under the DVS-CARR-MIDAS model. As shown in the figure, the long-run component evolves smoothly over time, effectively capturing persistent trends in volatility, while the short-run component typically reverts to a long-run level of 1.

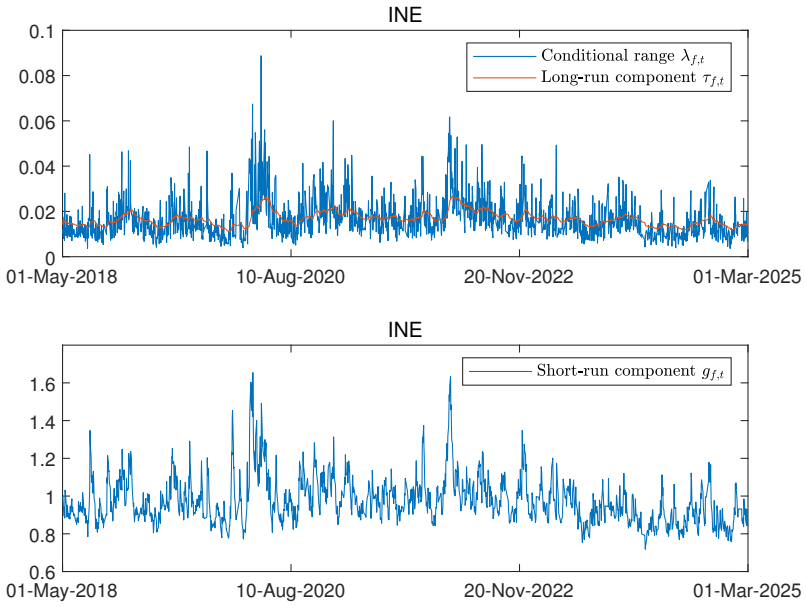

Figure 4. Conditional range (λ_t) and its long-term component (τ_t) and short-run component (g_t) from the DVS-CARR-MIDAS model.

According to Table 4, the proposed DVS-CARR-MIDAS model achieves the best in-sample fit among all specifications, with the highest log-likelihood value (5047.54). This superior performance highlights the importance of incorporating structural dynamic spillover effects from the dominant market when modeling China's crude oil futures volatility.

Table 4 links these breakpoints to major macroeconomic or energy-related events that likely triggered regime shifts. The coefficients κ_j quantify the time-varying impact of US volatility on the Chinese oil futures market. Positive values indicate that volatility in the US amplified fluctuations in the Chinese market, while negative values suggest a dampening effect.

Table 4. Structural breakpoints and relevant economic events.

Break ID	Break Date	κ_j	Effect	Associated Economic Event
1	2018-11-09	3.73	Amplifying	US-China trade tensions escalated
2	2019-01-09	-4.31	Dampening	China launched economic stimulus measures
3	2020-03-05	1.90	Amplifying	COVID-19 spreads globally, demand collapses
4	2020-05-07	1.37	Amplifying	US oil prices briefly turn negative (WTI futures crash)
5	2020-11-11	-1.93	Dampening	Chinese record crude import surge for stockpiling
6	2021-11-24	0.09	Mild Amplifying	US-led coordinated SPR release to ease global prices
7	2022-12-12	0.20	Mild Amplifying	China announced reopening policy signals
8	2024-02-02	1.29	Amplifying	US tech stock rally intensified
9	2025-02-28	-1.13	Dampening	China imposes new fuel tax policy impacting teapot refiners

Several breakpoints are particularly noteworthy due to the magnitude or sign of the spillover effects. For instance, $\kappa_3 = 1.90$ on 2020-03-05 reflects a strong amplifying effect during the global outbreak of COVID-19. Although the pandemic originated in China, global market panic intensified after major disruptions in the US, leading to a crash in WTI prices that transmitted heightened volatility to the China's market. Conversely, $\kappa_2 = -4.31$ on 2019-01-09 shows that volatility from the US had a stabilizing effect on the Chinese market, potentially due to positive sentiment driven by Chinese economic stimulus measures. Other events, such as the US strategic petroleum reserve (SPR) release on 2021-11-24 ($\kappa_6 = 0.09$), produced only mild spillover, implying that the presence of broad international policy coordination can help moderate spillover effects from the US crude oil futures market.

Overall, these results highlight that volatility spillovers are time-varying in magnitude and direction of influence (amplifying vs. dampening), shaped by event-specific market responses.

3.3. Out-of-sample results

For market participants, the out-of-sample forecasting performance of volatility models is of greater practical relevance. In this study, the in-sample period spans from May 2, 2018, to December 31, 2021, which is used for model estimation. The subsequent period from January 4, 2022, to February 28, 2025, is reserved for out-of-sample evaluation.

To generate volatility forecasts, we adopt a rolling window approach. Specifically, the procedure is as follows. First, we estimate each model using data from May 2, 2018, to December 31, 2021, and generate a one-step-ahead forecast for the volatility on the next trading day. Then, we move the estimation window forward by one day, keeping the window length fixed. For example, the model is re-estimated using data from May 3, 2018, to January 4, 2022, and a new one-step-ahead forecast is produced. This rolling estimation and forecasting process continues until the end of the sample period. Additionally, to assess forecast accuracy, we apply the four loss functions introduced in Section 2.8.1, including MAE, MSE, MAPE, and QLIKE.

Figure 5 presents the out-of-sample volatility forecasts for Chinese crude oil futures from the proposed DVS-CARR-MIDAS model and competing specifications. All models capture the broad dynamics of volatility, but their forecasting accuracy differs across periods. Table 5 reports the out-of-sample performance under four loss functions. The CARR-MIDAS model outperforms the baseline CARR model, showing that incorporating mixed-frequency information improves forecasts

by capturing long-memory features of volatility. The VS-CARR-MIDAS model, which includes a constant spillover effect from the US market, further enhances accuracy, underscoring the role of international volatility transmission. The DVS-CARR-MIDAS model delivers the best overall performance across all loss functions. By allowing spillover intensity to vary across regimes, it captures dynamic cross-market effects more effectively, demonstrating the value of jointly modeling MIDAS components and dynamic spillovers.

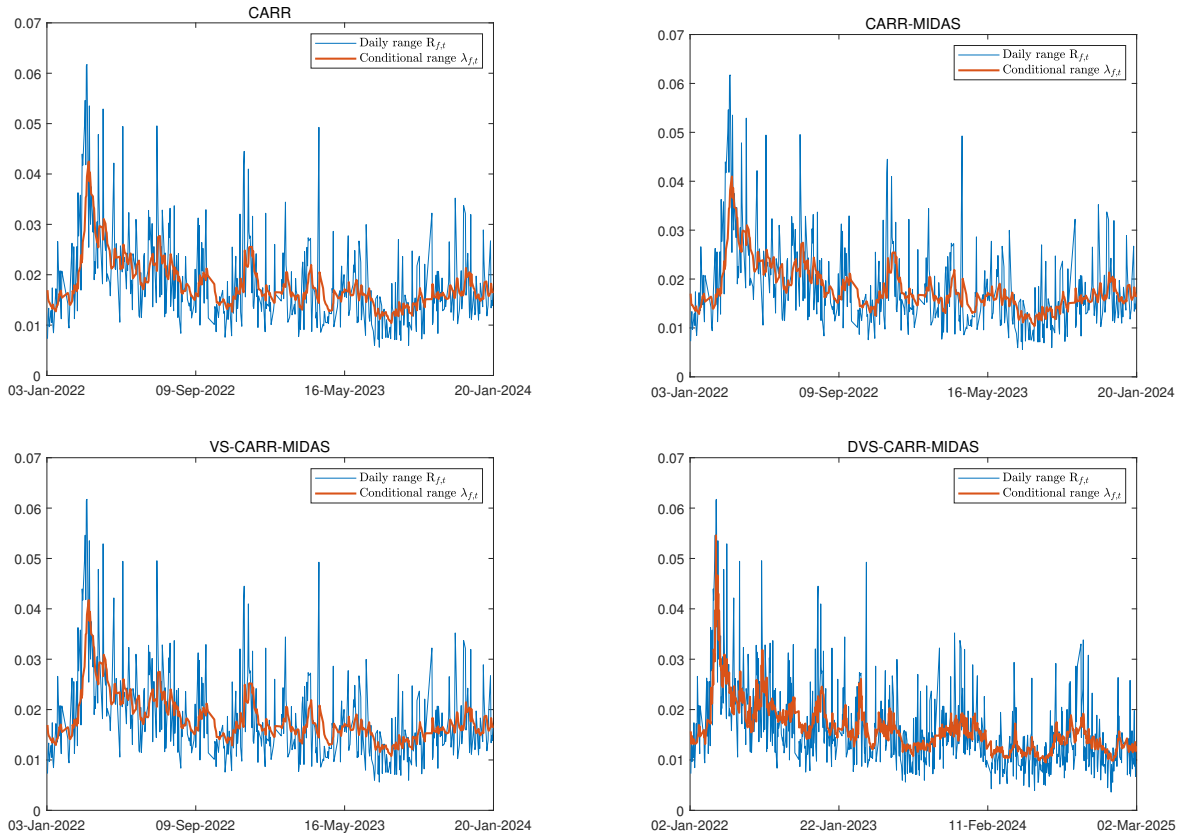

Figure 5. Out-of-sample forecast results of conditional variance for China's crude oil market.

Table 5. Volatility forecast evaluation results.

	CARR	CARR-MIDAS	VS-CARR-MIDAS	DVS-CARR-MIDAS
MAE	4.9405E-03	4.9266E-03	4.8883E-03	**4.5558E-03**
MSE	4.5267E-05	4.5325E-03	4.5019E-05	**3.8635E-05**
MAPE	3.4242E-01	3.4064E-01	3.3251E-01	**3.1702E-01**
QLIKE	7.9588E-02	7.9162E-02	7.6256E-02	**6.9609E-02**

Note: Bold entries indicate the model with the lowest loss value.

Further, we assess the forecast performance of all models using the MCS procedure. As shown in Table 6, the DVS-CARR-MIDAS model is consistently retained in the MCS across all loss functions, indicating its superior and statistically robust out-of-sample forecasting performance.

Table 6. MCS test results.

	CARR	CARR-MIDAS	VS-CARR-MIDAS	DVS-CARR-MIDAS
MAE	0.0000	0.0000	0.0000	**1.0000**
MSE	0.0002	0.0002	0.0002	**1.0000**
MAPE	0.0000	0.0000	0.0000	**1.0000**
QLIKE	0.0000	0.0000	0.0000	**1.0000**

Note: The numbers in the table are the p-values from the MCS test. A p-value greater than 0.1 (the bold numbers) indicates that the model is included in the MCS, meaning it is a model with better predictive ability.

3.4. Robustness tests

For robustness, we further conduct a series of additional tests, including the Diebold-Mariano (DM) test, R^2_{oos}, different dominant markets, and alternative forecast windows.

3.4.1. DM test

To evaluate whether the predictive accuracy of two competing models differs significantly, we employ the DM test proposed by Diebold and Mariano [26]. The test is based on the null hypothesis that the two forecasts have equal expected accuracy with respect to a specified loss function, and this hypothesis can be formally expressed as

$$H_0 : \mathbb{E}(d_{u,v}) = 0, \tag{3.1}$$

where $d_{uv,t}$ denotes the loss differential between model u and model v at time t. The DM test statistic is computed as

$$DM = \frac{\sqrt{M}\,\bar{d}}{\hat{\sigma}}, \tag{3.2}$$

where $\bar{d} = \frac{1}{M}\sum_{t=1}^{M} d_{uv,t}$ is the sample mean of the loss differential, and $\hat{\sigma}$ is the standard deviation estimator of $d_{uv,t}$.

Under the null hypothesis, the DM statistic follows an asymptotically standard normal distribution:

$$\frac{\sqrt{M}\,\bar{d}}{\hat{\sigma}} \xrightarrow{M\to\infty} N(0,1). \tag{3.3}$$

When H_0 is rejected, it indicates that the difference in forecasting accuracy between the two models is statistically significant.

Empirical results reported in Table 7 show that the DVS-CARR-MIDAS model consistently outperforms its competitors in out-of-sample forecasting across several loss functions, including MAE, MSE, MAPE, and QLIKE. The positive and statistically significant DM test statistics at the 10% level support the superior predictive performance of the DVS-CARR-MIDAS model.

Table 7. DM test results.

	CARR	CARR-MIDAS	VS-CARR-MIDAS
MAE loss function			
CARR-MIDAS	1.5409		
VS-CARR-MIDAS	3.12***	2.4466**	
DVS-CARR-MIDAS	6.3811***	6.0998***	5.4359***
MSE loss function			
CARR-MIDAS	0.3023		
VS-CARR-MIDAS	1.1488	1.3870	
DVS-CARR-MIDAS	4.8932***	4.6589***	4.5635***
MAPE loss function			
CARR-MIDAS	3.3011***		
VS-CARR-MIDAS	6.4292***	5.6501***	
DVS-CARR-MIDAS	7.1234***	6.7196***	4.2419***
QLIKE loss function			
CARR-MIDAS	2.3279**		
VS-CARR-MIDAS	5.4659***	4.9782***	
DVS-CARR-MIDAS	7.3202***	7.0741***	4.9104***

Note: A positive test statistic indicates that the model in the row outperforms the model in the column, and vice versa. The symbols *, **, and *** denote statistical significance at the 10%, 5%, and 1% levels, respectively. MAE, MSE, MAPE, and QLIKE represent the mean absolute error, mean absolute percentage error, root mean squared error, and quasi-likelihood loss, respectively.

3.4.2. R^2_{oos} test

We conduct the out-of-sample R^2_{oos} test to evaluate the forecast performance for robustness. Specifically, the out-of-sample R^2_{oos} is formulated as follows:

$$R^2_{\text{oos}} = 1 - \frac{\text{MSPE}_m}{\text{MSPE}_{bm}}, \tag{3.4}$$

$$\text{MSPE}_m = \frac{1}{M}\sum_{t=1}^{M}(R_t - \hat{R}_t^{(m)})^2, \tag{3.5}$$

$$\text{MSPE}_{bm} = \frac{1}{M}\sum_{t=1}^{M}(R_t - \hat{R}_t^{(bm)})^2, \tag{3.6}$$

where MSPE_m and MSPE_{bm} represent the mean squared prediction from the competing model and the benchmark model, as well as R_t, $\hat{R}_t^{(m)}$, and $\hat{R}_t^{(bm)}$ denoting the true range, the forecasted range from the model, and the forecasted range from the benchmark model, respectively. Then, we adopt the GARCH model as the benchmark model in this paper. It is obvious that a positive R^2_{oos} suggest that the competing model outperforms the benchmark model in predictive accuracy, as reflected by a lower MSPE.

To test the statistical significance of R^2_{oos}, we employ the MSPE-adjusted statistic, defined as

$$\hat{f}_t = (R_t - \hat{R}_t^{(bm)})^2 - (R_t - \hat{R}_t^{(m)})^2 + (\hat{R}_t^{(bm)} - \hat{R}_t^{(m)})^2. \tag{3.7}$$

The CW statistic is computed by regressing $\hat{f}_t$ on a constant.

Table 8 reports the out-of-sample evaluation results based on the R^2_{oos} test. All competing models yield significantly positive R^2_{oos} values, indicating improvements in MSPE over the benchmark CARR model. Among them, the DVS-CARR-MIDAS model achieves the highest R^2_{oos} value, together with the largest CW statistic and zero p-value, confirming its superior performance for Chinese crude oil futures volatility.

Table 8. MCS test results.

	R^2_{oos}%	CW statistic	p-value
CARR-MIDAS	0.13	1.0091	0.4964
VS-CARR-MIDAS	5.50	2.0680	0.0193
DVS-CARR-MIDAS	14.65	5.4857	0.0000

3.4.3. Alternative dominant crude oil futures market

Moreover, we consider replacing the WTI crude oil data with Brent crude oil data. Given that Brent serves as a major global benchmark and reflects broader international oil market conditions, this substitution allows us to examine whether the predictive performance remains consistent across alternative dominant crude oil markets.

Table 9. Volatility forecast evaluation results: different dominant markets.

	CARR	CARR-MIDAS	VS-CARR-MIDAS	DVS-CARR-MIDAS
MAE	4.9197E-03	4.9077E-03	4.8544E-03	**4.5245E-03**
MSE	6.0138E-05	6.0152E-05	5.9739E-05	**3.8106E-05**
MAPE	3.3968E-01	3.3805E-01	3.2930E-01	**3.1419E-01**
QLIKE	7.8476E-02	7.8084E-02	7.5173E-02	**6.8151E-02**

Note: Bold entries indicate the model with the lowest loss value.

Table 10. MCS test results.

	CARR	CARR-MIDAS	VS-CARR-MIDAS	DVS-CARR-MIDAS
MAE	0.0000	0.0000	0.0000	**1.0000**
MSE	0.0008	0.0008	0.0008	**1.0000**
MAPE	0.0000	0.0000	0.0000	**1.0000**
QLIKE	0.0000	0.0000	0.0000	**1.0000**

Note: The numbers in the table are the p-values from the MCS test. A p-value greater than 0.1 (the bolded numbers) indicates that the model is included in the MCS, meaning it is a model with better predictive ability.

As shown in Table 9, the DVS-CARR-MIDAS model continues to deliver the lowest forecast errors across all loss metrics, consistent with the earlier findings. The MCS results in Table 10 further confirm its robustness, with DVS-CARR-MIDAS being the only model included in the 90% confidence set across all evaluation criteria. These results demonstrate the robustness of our model's forecasting performance across alternative dominant crude oil markets.

3.4.4. Different out-of-sample forecast windows

To further evaluate the robustness of the forecasting results, we evaluate each model over out-of-sample windows of 120, 240, and 480 trading days, corresponding to approximately half-year, one-year, and two-year horizons.

Table 11 reports the volatility forecasting results under different out-of-sample forecast windows. Across all windows (120, 240, and 480 days), the DVS-CARR-MIDAS model consistently achieves the lowest loss values under all four evaluation metrics. These results highlight the robustness of the model in capturing volatility dynamics over both short-term and long-term forecast periods.

Table 11. Volatility forecast evaluation results: different prediction windows.

	CARR	CARR-MIDAS	VS-CARR-MIDAS	DVS-CARR-MIDAS
		prediction windows : 120 days		
MAE	7.2455E-03	7.2631E-03	7.2248E-03	**6.1051E-03**
MSE	9.3507E-05	9.4508E-05	9.3281E-05	**7.4746E-05**
MAPE	3.1053E-01	3.1076E-01	3.0961E-01	**2.7055E-01**
QLIKE	6.7897E-02	6.8087E-02	6.7489E-02	**5.4325E-02**
		prediction windows : 240 days		
MAE	6.3356E-03	6.3486E-03	6.3341E-03	**5.8961E-03**
MSE	7.2566E-05	7.3257E-05	7.2584E-05	**6.0913E-05**
MAPE	3.1490E-01	3.1542E-01	3.1443E-01	**3.0088E-01**
QLIKE	6.9152E-02	6.9512E-02	6.8802E-02	**6.2710E-02**
		prediction windows : 480 days		
MAE	5.4844E-03	5.4829E-03	5.4962E-03	**5.0326E-03**
MSE	5.5676E-05	5.5901E-05	5.5669E-05	**4.7282E-05**
MAPE	3.2076E-01	3.2045E-01	3.2288E-01	**2.9567E-01**
QLIKE	7.1429E-02	7.1391E-02	7.1862E-02	**6.2459E-02**

Note: Bold entries indicate the model with the lowest loss value.

3.5. Economic value of volatility timing

This paper evaluates the economic value of volatility forecasts by assessing their contribution to portfolio allocation performance. We adopt a mean-variance framework in which the optimal portfolio weight is derived conditional on the volatility predictions. Specifically, assuming that an investor makes decisions based on conditional mean-variance optimization, the utility function is defined as

$$U_t(r_{p,t+1}) = E[r_{p,t+1}|\Phi_t] - \frac{A}{2}Var[r_{p,t+1}|\Phi_t], \tag{3.8}$$

where $r_{p,t+1}$ denotes the portfolio return, A is the coefficient of risk aversion, and $E[r_{p,t+1}|\Phi_t]$ and $Var[r_{p,t+1}|\Phi_t]$ are the conditional mean and variance of the portfolio return, respectively. By maximizing $U_t(r_{p,t+1})$, the optimal weight allocated to the risky asset is obtained as

$$w_t^* = \frac{E[r_{t+1}|\Phi_t] - r_{c,t+1}}{AVar[r_{t+1}|\Phi_t]}, \tag{3.9}$$

where r_{t+1} is the return of the risky asset (INE crude oil futures), $r_{c,t+1}$ is the risk-free rate, and $E[r_{t+1}|\Phi_t]$ and $Var[r_{t+1}|\Phi_t]$ are the conditional mean and variance of the risky asset return, respectively. The three-month Shanghai Interbank Offered Rate (SHIBOR) is used as a proxy for the risk-free rate, while the expected return of the risky asset is estimated using a rolling-sample average. The conditional variance of the risky asset return is provided by volatility forecasts from the models considered in this paper (i.e., the DVS-CARR-MIDAS model and its competing specifications). To avoid excessive leverage and reflect realistic trading conditions, we impose the constraint $0 \leq w_t^* \leq 1.5$. Given the optimal weight, the realized portfolio return is calculated as

$$r_{p,t+1} = r_{c,t+1} + w_t^*(r_{t+1} - r_{c,t+1}). \tag{3.10}$$

To evaluate the performance of competing volatility models, we employ a utility-based comparison. Following Fleming et al. (2003) [27], we use the average realized utility to compare competing strategies against a benchmark. The average realized utility is expressed as

$$\bar{U}(r_p) = \frac{1}{T}\sum_{t=0}^{T-1}\left(r_{p,t+1} - \frac{A}{2}\left(r_{p,t+1} - \frac{1}{T}\sum_{t=0}^{T-1} r_{p,t+1}\right)^2\right). \tag{3.11}$$

To further quantify the incremental economic benefit of each model, we compute the performance fee, defined as the additional fee an investor would be willing to pay in order to switch from the benchmark to the competing strategy:

$$\Delta = \bar{U}(r_p) - \bar{U}(r_{p,bm}), \tag{3.12}$$

where $\bar{U}(r_{p,bm})$ denotes the average realized utility under the benchmark model.

For robustness, we also report the Sharpe ratio (SR) as an alternative measure of portfolio performance:

$$\text{SR} = \frac{E[r_{p,t+1|\Phi_t}] - r_{c,t+1}}{\sqrt{Var[r_{p,t+1|\Phi_t}]}}. \tag{3.13}$$

A higher SR indicates greater excess return per unit of risk, thus reflecting higher economic value of the volatility forecasts.

In the empirical analysis, we take the standard CARR model as the benchmark and evaluate portfolio performance under different levels of investor risk aversion ($A = 3, 6, 9$). Table 12 reports annualized performance fees and Sharpe ratios across models. The results show that all three extended specifications (CARR-MIDAS, VS-CARR-MIDAS, and DVS-CARR-MIDAS) deliver positive performance fees, with the DVS-CARR-MIDAS consistently ranking highest. Specifically, its performance fees range from 35 to 106 basis points, followed by the VS-CARR-MIDAS model (30 to 92 basis points). These findings highlight that explicitly incorporating dynamic volatility spillovers from the US oil market substantially enhances the economic value of volatility forecasts. Moreover,

the DVS-CARR-MIDAS model also attains the highest Sharpe ratios, confirming its superior portfolio performance. Overall, the evidence suggests that modeling dynamic cross-market spillovers yields robust improvements across different levels of risk aversion.

Table 12. The performance of the investment portfolio.

	$A = 3$		$A = 6$		$A = 9$	
	Δ	SR	Δ	SR	Δ	SR
CARR	-	0.2500	-	0.1512	-	0.1226
CARR-MIDAS	72.2710	0.2820	48.2103	0.1697	24.0903	0.1369
VS-CARR-MIDAS	92.1154	0.3700	61.4440	0.2236	30.7051	0.1809
DVS-CARR-MIDAS	**106.9250**	**0.4360**	**71.2913**	**0.2640**	**35.6417**	**0.2139**

Note: Bold entries indicate the model with the highest economic value.

4. Conclusions

This paper proposes a range-based dynamic volatility spillovers CARR-MIDAS (DVS-CARR-MIDAS) model to forecast volatility in the Chinese crude oil futures market. The model integrates daily range information and allows the spillover intensity from the dominant US crude oil market to vary across structural regimes. Empirically, we find that spillovers from the US to the Chinese crude oil futures market are significant and time-varying, alternating between amplifying and dampening across regimes. The DVS-CARR-MIDAS model delivers superior in-sample fit and out-of-sample forecasts relative to competing CARR-type benchmarks, with robustness confirmed by the DM test, the R^2_{oos} test, alternative specifications of the dominant market, and different forecast horizons. Moreover, an economic-value analysis shows that the model provides meaningful portfolio benefits.

These findings align with a strand of recent research that documents time-varying volatility transmission across markets when flexible, time-adaptive methods are used. In particular, prior work that employs time-varying parameter and dynamic connectedness frameworks has similarly emphasized that volatility spillovers evolve over time and respond to changing market conditions. Our results complement that literature by demonstrating consistent time variation in cross-market volatility transmission when a range-based, MIDAS-type approach is employed.

At the same time, our approach departs from studies that focus on frequency-domain or time-frequency decompositions of spillovers. The key novelty of this paper is the explicit incorporation of structural regime shifts into a range-based CARR-MIDAS framework and the estimation of regime-dependent spillover coefficients. By externally identifying breakpoints in the dominant market and allowing spillover parameters to change across these regimes, the model captures sudden structural changes in transmission intensity while still exploiting both short-run and long-run information through the MIDAS structure. This combination of range-based intraday information, mixed-frequency long-run drivers, and regime-dependent spillover dynamics distinguishes our contribution methodologically.

The contributions of this study can be summarized along three dimensions. First, methodologically, this study advances beyond static spillover models by incorporating regime-dependent spillover coefficients, which enable the transmission intensity from the dominant market to vary across different structural states. Second, from a practical perspective, the findings provide valuable implications for

policymakers and market participants. Understanding how spillovers vary across regimes can inform risk management practices and portfolio allocation strategies, while also shedding light on the price discovery process between US and Chinese oil futures. Third, the modeling framework is general and can be extended to other commodity markets (e.g., metals, agricultural products) or financial assets (e.g., equities, exchange rates), thereby offering a versatile tool for future empirical research.

For future research, this study could be extended to examine higher-moment spillovers, which have gained attention in recent work (He and Hamori [28, 29]).

Author contributions

Xinyu Wu: Conceptualization, Methodology, Writing–review & editing, Funding acquisition, Supervision, Data curation; Yuanzheng Liu: Formal analysis, Writing–original draft, Software; Junlin Pu: Writing–review & editing, Software; Xiaona Wang: Funding acquisition, Visualization. All authors have read and agreed to the published version of the manuscript.

Use of Generative-AI tools declaration

The authors declare they have not used Artificial Intelligence (AI) tools in the creation of this article.

Acknowledgments

This research is supported by the National Natural Science Foundation of China under Grant No. 71971001; Natural Science Foundation of Anhui Province under Grant No. 2208085Y21; Academic Funding Project for Top Academic Talents in Anhui Universities under Grant No. gxbjZD2022019; Outstanding Youth Research Project for Anhui Universities under Grant No. 2022AH020047; Excellent Scientific Research and Innovation Team for Anhui Universities under Grant No. 2022AH010045; Innovative Research Project for Graduates of Anhui University of Finance and Economics under Grant No. ACYC2023132; Academic Innovation of Graduate Students in Anhui Province under Grant No. 2024xscx087; The Youth Scholars Development Program for Anhui Province Federation of Social Sciences under Grant No. QNXR2024101; and Scientific Research Project for Tongling University under Grant No. 2024tlxysk04.

Conflict of interest

The authors certify that there is no actual or potential conflict of interest in relation to this article.

References

1. F. Ma, C. Liang, Y. H. Ma, M. I. M. Wahab, Cryptocurrency volatility forecasting: a Markov regime-switching MIDAS approach, *J. Forecast.*, **39** (2020), 1277–1290. https://doi.org/10.1002/for.2691
2. F. Ma, C. Liang, Q. Zeng, H. B. Li, Jumps and oil futures volatility forecasting: a new insight, *Quant. Finance*, **21** (2021), 853–863. https://doi.org/10.1080/14697688.2020.1805505

3. C. Q. Luo, Y. Qu, Y. Y. Su, L. Dong, Risk spillover from international crude oil markets to China's financial markets: evidence from extreme events and US monetary policy, *N. Am. J. Econ. Finance*, **70** (2024), 102041. https://doi.org/10.1016/j.najef.2023.102041

4. M. Liu, C. C. Lee, Capturing the dynamics of the China crude oil futures: Markov switching, co-movement, and volatility forecasting, *Energy Econo.*, **103** (2021), 105622. https://doi.org/10.1016/j.eneco.2021.105622

5. C. W. Sun, J. L. Min, J. C. Sun, X. Gong, The role of China's crude oil futures in world oil futures market and China's financial market, *Energy Econ.*, **120** (2023), 106619. https://doi.org/10.1016/j.eneco.2023.106619

6. T. Su, B. Q. Lin, Reassessing the information transmission and pricing influence of Shanghai crude oil futures: a time-varying perspective, *Energy Econ.*, **140** (2024), 107977. https://doi.org/10.1016/j.eneco.2024.107977

7. Z. K. Zhang, Y. D. Wang, J. H. Xiao, Y. J. Zhang, Not all geopolitical shocks are alike: identifying price dynamics in the crude oil market under tensions, *Resour. Policy*, **80** (2023), 103238. https://doi.org/10.1016/j.resourpol.2022.103238

8. Y. Y. Yang, Y. R. Ma, M. Hu, D. Y. Zhang, Q. Ji, Extreme risk spillover between Chinese and global crude oil futures, *Finance Res. Lett.*, **40** (2021), 101743. https://doi.org/10.1016/j.frl.2020.101743

9. X. H. Huang, S. P. Huang, Identifying the comovement of price between China's and international crude oil futures: a time-frequency perspective, *Int. Rev. Financ. Anal.*, **72** (2020), 101562. https://doi.org/10.1016/j.irfa.2020.101562

10. J. P. Li, M. Umar, J. L. Huo, The spillover effect between Chinese crude oil futures market and Chinese green energy stock market, *Energy Econ.*, **119** (2023), 106568. https://doi.org/10.1016/j.eneco.2023.106568

11. Z. F. Dai, H. Y. Zhu, Time-varying spillover effects and investment strategies between WTI crude oil, natural gas and Chinese stock markets related to belt and road initiative, *Energy Econ.*, **108** (2022), 105883. https://doi.org/10.1016/j.eneco.2022.105883

12. Y. Jin, H. Zhao, L. Bu, D. Y. Zhang, Geopolitical risk, climate risk and energy markets: a dynamic spillover analysis, *Int. Rev. Financ. Anal.*, **87** (2023), 102597. https://doi.org/10.1016/j.irfa.2023.102597

13. L. B. Salem, M. Zayati, R. Nouira, C. Rault, Volatility spillover between oil prices and main exchange rates: evidence from a DCC-GARCH-connectedness approach, *Resour. Policy*, **91** (2024), 104880. https://doi.org/10.1016/j.resourpol.2024.104880

14. M. Parkinson, The extreme value method for estimating the variance of the rate of return, *J. Bus.*, **53** (1980), 61–65.

15. R. Y. Chou, Forecasting financial volatilities with extreme values: the conditional autoregressive range (CARR) model, *J. Money Credit Banking*, **37** (2005), 561–582.

16. Y. He, A. Han, Y. M. Hong, Y. Y. Sun, S. Y. Wang, Forecasting crude oil price intervals and return volatility via autoregressive conditional interval models, *Econ. Rev.*, **40** (2021), 584–606. https://doi.org/10.1080/07474938.2021.1889202

17. B. Wang, Y. X. Qian, E. P. Yu, Bayesian analysis for functional coefficient conditional autoregressive range model with applications, *Econ. Model.*, **144** (2025), 107003. https://doi.org/10.1016/j.econmod.2024.107003

18. S. K. Tan, K. H. Ng, J. S. K. Chan, Predicting returns, volatilities and correlations of stock indices using multivariate conditional autoregressive range and return models, *Mathematics*, **11** (2023), 1–24. https://doi.org/10.3390/math11010013

19. X. Y. Wu, H. B. Xie, H. M. Zhang, Time-varying risk aversion and renminbi exchange rate volatility: evidence from CARR-MIDAS model, *N. Am. J. Econ. Finance*, **61** (2022), 101703. https://doi.org/10.1016/j.najef.2022.101703

20. X. Y. Wu, H. Cui, L. Wang, Forecasting oil futures price volatility with economic policy uncertainty: a CARR-MIDAS model, *Appl. Econ. Lett.*, **30** (2023), 120–125. https://doi.org/10.1080/13504851.2021.1977232

21. X. V. Vo, T. T. A. Tran, Modelling volatility spillovers from the US equity market to ASEAN stock markets, *Pac. Basin Finance J.*, **59** (2020), 101246. https://doi.org/10.1016/j.pacfin.2019.101246

22. G. T. H. Vuong, M. H. Nguyen, A. N. Q. Huynh, Volatility spillovers from the Chinese stock market to the U.S. stock market: the role of the COVID-19 pandemic, *J. Econ. Asymmetries*, **26** (2022), e00276. https://doi.org/10.1016/j.jeca.2022.e00276

23. C. Inclan, G. C. Tiao, Use of cumulative sums of squares for retrospective detection of changes of variance, *J. Amer. Statist. Assoc.*, **89** (1994), 913–923. https://doi.org/10.1080/01621459.1994.10476824

24. P. R. Hansen, A. Lunde, J. M. Nason, The model confidence set, *Econometrica*, **79** (2011), 453–497. https://doi.org/10.3982/ECTA5771

25. D. Kwon, The impacts of oil price shocks and United States economic uncertainty on global stock markets, *Int. J. Finance Econ.*, **27** (2022), 1595–1607. https://doi.org/10.1002/ijfe.2232

26. F. X. Diebold, R. S. Mariano, Comparing predictive accuracy, *J. Bus. Econom. Statist.*, **20** (2002), 134–144. https://doi.org/10.1198/073500102753410444

27. J. Fleming, C. Kirby, B. Ostdiek, The economic value of volatility timing using "realized" volatility, *J. Financ. Econ.*, **67** (2003), 473–509. https://doi.org/10.1016/S0304-405X(02)00259-3

28. X. He, S. Hamori, The higher the better? Hedging and investment strategies in cryptocurrency markets: insights from higher moment spillovers, *Int. Rev. Financ. Anal.*, **95** (2024), 103359. https://doi.org/10.1016/j.irfa.2024.103359

29. X. He, S. Hamori, Is volatility spillover enough for investor decisions? A new viewpoint from higher moments, *J. Int. Money Finance*, **116** (2021), 102412. https://doi.org/10.1016/j.jimonfin.2021.102412

AIMS Press